Exp Brain Res (2004) 155: 485–499
DOI 10.1007/s00221-003-1755-3

RESEARCH ARTICLES

S. Shuichi Haupt · Friederike Spengler · Robert Husemann · Hubert R. Dinse

Receptive field scatter, topography and map variability in different layers of the hindpaw representation of rat somatosensory cortex

Received: 4 April 2003 / Accepted: 16 October 2003 / Published online: 27 January 2004
© Springer-Verlag 2004

Abstract We recorded neurons extracellularly in layers II/III, IV, and V of the hindpaw representation of primary somatosensory cortex in anesthetized rats and studied laminar features of receptive fields (RFs) and representational maps. On average, RFs were smallest in layer IV and largest in layer V; however, for individual penetrations we found substantial deviations from this rule. Within the hindpaw representation, a distinct rostrocaudal gradient of RF size was present in all layers. While layer V RFs were generally largest independent of this gradient, layer IV RFs recorded caudally representing the proximal portions of the paw were larger than layer II/III RFs recorded rostrally representing the digits. The individual scatter of the locations of RFs across laminar groups was in the range of several millimeters, corresponding to about 25% of the average RF diameter. The cutaneous representations of the hindpaw in extragranular layers were confined to the areal extent defined by responsive sites in layer IV. Comparison between RFs determined quantitatively and by handplotting showed a reliable correspondence. Repeated measurements of RFs revealed spontaneous fluctuations of RF size of no more than 5% of the initial condition over an observation period of several hours. The topography and variability of cortical maps of the hindpaw representation were studied with a quantitative interpolation method taking into account the geometric centers of RFs and the corresponding cortical recording sites. On average, the overall topography in terms of preservation of neighborhood relations was present in all layers, although some individual maps showed severe distortions of topography. Factors contributing to map variability were overall position of the representation on the cortical surface, internal topography and spatial extent. Interindividual variability of map layout was always highest in the digit representations. Local topographic orderliness was lowest in layer V, but comparable in layers II/III and IV. Within layer IV, the lowest orderliness was observed in the digit representations. Our data emphasize a substantial variability of RF size, overlap and position across layers and within layers. At the level of representational maps, we found a similar degree of variability that often co-varied across layers, with little evidence for significant layer specificity. Laminar differences are likely to arise from the specific input-output pattern, layer-specific cell types and the connectivity between different layers. Our findings emphasizing similarities in the variability across layers support the notion of tightly coupled columnar interactions between different layers.

Keywords Cortical layers · Individual variability · Topography · Quantitative reconstruction of maps · Orderliness

S. S. Haupt · F. Spengler · R. Husemann · H. R. Dinse (✉)
Institute for Neuroinformatics, Department of Theoretical Biology, Ruhr University Bochum,
ND 04, 44780 Bochum, Germany
e-mail: hubert.dinse@neuroinformatik.ruhr-uni-bochum.de
Tel.: +49-234-3225565
Fax: +49-234-3214209

S. S. Haupt
Department of Mechano-Informatics, Faculty of Engineering, University of Tokyo,
7-3-1 Hongo, Bunkyo-ku,
113 Tokyo, Japan

Present address:
S. S. Haupt
Institute for Ecology, Faculty VII, Technical University Berlin FR 1-1,
Franklinstr. 28/29,
10587 Berlin, Germany

Introduction

A striking structural principle of neocortical organization is its homogeneity in the tangential plane, and inhomogeneity perpendicular to it. The appearance of laminated patterns is due to the distribution of specific cell types (Peters and Jones 1984). Another anisotropy in the vertical comes from the fact that different layers receive their input from different principal sources, and in turn distribute information to different targets (Jones and Powell 1970;

Burkhalter 1989). Consequently, response properties of a neuron depend to a large extent on the layer it belongs to (Schiller et al. 1976; Gilbert 1977; Simons 1978; Henry et al. 1979; Simons and Woolsey 1979; Lamour et al. 1983a; Chapin 1986). From a theoretical point of view, such an organization can be considered as a multi-input-multi-output system (Krone et al. 1986; Kyriazi and Simons 1993).

This structural framework is similar in different sensory cortices (Rockel et al. 1980; for review see Schüz and Miller 2002). In rodent SI, terminals of thalamocortical projections are most frequently found in layer IV, but to a minor extent also in lower layers III, V and VI (Herkenham 1980; Keller et al. 1985; Jensen and Killackey 1987; Chapin and Lin 1990). The majority of cortico-cortical efferents stems from supragranular layers, whereas cortico-subcortical efferents originate from infragranular layers. However, the total number of afferent synapses, even in layer 4, comprises only a small fraction of the total number of synapses indicative that the amount of intracortical processing outweighs the impact of feedforward afferent-mediated processing (Kyriazi and Simons 1993; for review see Sherman and Guillary 2001), although the functional signature of recurrent processing is difficult to trace and therefore still is a matter of debate (Miller et al. 2001).

Despite the prominent laminated structure, most of the current knowledge about processing in sensory cortices has been obtained from recordings in layer IV, particularly in terms of topography of representations. Extragranular layers are assumed to mirror the topography found in granular layers due to the columnar organization, although receptive field properties differ with respect to laminar position. Therefore, there is a strong need for information about lamina-specific properties at the level of entire representations.

In addition, sensory representations are known to display a considerable individual variability that must be taken into account when investigating sensory maps and their plastic reorganizational properties. For example, considerable variability has been described for the hand representation in somatosensory cortex of monkeys (Merzenich et al. 1987) and for the rat barrel field (Riddle and Purves 1995; Chen-Bee and Frostig 1996). It remains to be clarified which geometric properties of representations such as absolute location and spatial extent contribute to the overall variability observed.

We therefore aimed to characterize the hindpaw representation of the rat primary somatosensory cortex and its individual variability comparatively in three laminar groups using extracellular recordings of multiunit activity. We studied the relationship between laminar organization and receptive field properties and entire representational maps; the latter were visualized using a computer-based interpolation algorithm. These studies were also motivated by an upcoming study on layer dependence of plasticity, for which the understanding of variability and stability of processing in different layers is paramount.

Materials and methods

Animal preparation and anesthesia

Experiments were performed in 29 adult Sprague-Dawley rats of both sexes. Animals were anesthetized with an initial dose of 1.5 mg/g body weight urethane (Sigma, 20% in water, i.p.). Additional anesthetic (1/8 of the initial quantum) was administered when eye-blinking or paw-withdrawal reflexes could be elicited. Treatment of all animals was within the guidelines of the National Institution of Health Guide and Care for Use of Laboratory Animals (Revised 1987); all experiments were approved by the German Animal Care and Use Committee. The cisterna magna was drained to prevent swelling of the cortex. After an unilateral craniotomy and resection of the dura, the cortex was covered with warm silicone oil (DC 200 50cst, Serva). Rectal temperature was kept at 37°C using a feedback-controlled heating pad. The ECG and respiration rate were stable throughout every individual experiment.

Electrophysiology

Glass micropipettes with a tip diameter of 10 μm (OD) filled with 3 M NaCl or Chicago Sky Blue (Sigma, 2% w/v) in 0.5 M sodium acetate (2 MΩ at 10 kHz) and a low impedance reference electrode fixed to the neck muscles were used for recording. To reduce variability of recording conditions, electrode tip size was meticulously controlled by breaking tips to a defined size under microscopic control (×200). A total of 502 penetrations were made perpendicular to the cortical surface within the hindpaw representations of the primary somatosensory cortex using a motor micro drive (1 μm resolution) to advance the electrodes. Multi-unit activity was recorded at 300–400 μm (supragranular, corresponding to layer II/III), 700 μm (layer IV), and 1,050–1,150 μm (infragranular, layer V) subpial depth. In the superficial laminae, there was usually very low spontaneous activity. In contrast, high levels of spontaneous activity were typically found in infragranular recordings, where spike amplitude served as a characteristic indicator. The action potentials discriminated were clearly above background. Accordingly, the multiunit recordings consisted of a small number of action potentials, most likely somatic in nature because of the spike durations. The repeated recordings in more than 200 of our sample of approximately 1,200 recoding sites revealed very few fluctuations (2–6%), which is an indication that variability due to fluctuations in the number of recorded neurons in the multiunit cluster is unlikely to have a major effect on RF size. As a rule, for each penetration, one RF per laminar group was recorded, except for those cases in which unresponsive sites were encountered. Penetrations were spaced at irregular intervals of 100–200 μm according to the vascular patterns and were marked in digitized pictures of the cortical surface in stereotaxic coordinates.

Tactile stimulation and RF assessment

On average, in each animal, 10–25 cutaneous receptive fields (RFs) per laminar group were identified on the ventral side of the hindpaw. RF size was determined by handplotting using von-Frey filaments for evoking cutaneous responses (0.2 mm diameter, applying a force of 80 mN). RFs were defined as all locations on the skin, where clearly discernable spike responses above spontaneous activity were reliably elicited by low-amplitude repetitive tactile stimulation at ~1/s. This definition differs from center or minimal RFs often used in handplotting experiments (cf. Merzenich et al. 1984; Recanzone et al. 1992). Non-cutaneous (deep-input) RFs were infrequently encountered and were not included for further analyses. RF size was calculated by computerized planimetry; location of RFs is given by geometric RF centers. Using a bitmap in which the pixels belonging to the RF are labeled by a particular value, the coordinates of the RF pixels were averaged. Overlap between RFs was

expressed as the absolute overlap in mm^2 between two RFs normalized with respect to the size of one of the RF pair.

In order to study RF organization quantitatively, we modified the so-called response plane technique by recording neuronal responses to computer-controlled tactile stimulation at up to 20 different locations on the hindpaw. For each location, PSTHs were calculated from neural responses evoked by a solenoid-driven mechanical stimulator with a tip size of 1.5 mm (duration of tactile stimuli 8 ms applied at a frequency of 1 Hz, responses of 32 sweeps accumulated) and response planes were constructed (cf. Godde et al. 1996).

Reconstruction of cortical maps

The systematic representations of the sensory epithelium is a key feature of cortical and subcortical organization. They have in common that the neighborhood relationships of the outside physical world are preserved in the arrangement of cortical or subcortical representations. The outcome is a topographic map of the physical world. To evaluate quantitatively cortical maps and their inter-individual variability, quantitative measures that capture the degree of topographic order are needed. We present an interpolation algorithm, which allows the computation of peripheral coordinates of the hindpaw according to their cortical representational locations.

The mapping algorithm utilized was originally developed for maps of the visual field in the superior colliculus (Quevedo et al. 1996) and was adapted to rat somatosensory cortex (Spengler et al. 1995). Coordinates of the cortical penetration sites (u, v) and of the geometric centers of the corresponding RFs (x, y) were used for quantitative reconstruction of representational maps of the hindpaw. The reconstruction is based on the construction of a rectilinear grid on the hindpaw that is projected onto the cortical surface assuming a bijective projection. A linear approximation L:

$$L_{x,y} := \begin{pmatrix} x \\ y \end{pmatrix} \rightarrow \begin{pmatrix} u \\ v \end{pmatrix} = \begin{pmatrix} a(x,y) & b(x,y) \\ c(x,y) & d(x,y) \end{pmatrix} \begin{pmatrix} x \\ y \end{pmatrix} + \begin{pmatrix} u_0 \\ v_0 \end{pmatrix} \quad with \begin{pmatrix} u_0 \\ v_0 \end{pmatrix} = L_{x=0,y=0} \tag{1}$$

is used to determine any point (u, v) on the cortical surface corresponding to a point (x, y) on the paw. L is used to minimize a term describing a locally weighted error, E, defined as:

$$E(x,y) := \sum_{i=1}^{n} \left\| \begin{pmatrix} u_i \\ v_i \end{pmatrix} - L_{x,y}\begin{pmatrix} x_i \\ y_i \end{pmatrix} \right\|^2 e^{-\left(\frac{1}{2\sigma^2}\left\| \begin{pmatrix} x \\ y \end{pmatrix} - \begin{pmatrix} x_i \\ y_i \end{pmatrix} \right\|^2\right)} \quad with\, \sigma = \frac{d_{\min 1} + d_{\min 2}}{2}, \tag{2}$$

where $d_{\min 1}$ is the distance between the point (x, y) for which the cortical location is to be approximated and the nearest recorded RF center and $d_{\min 2}$ the same distance but to the second-nearest actual RF center. The minimization of the error term (Eq. 2) is done separately for each coordinate by solving the systems of partial derivatives with respect to a, b, and u_0 (for x/u coordinate) and c, d, and v_0 (for y/v coordinate) for finding their zero crossings. The set of equations results in a 3×3 matrix that is solved by singular value decomposition. This procedure corresponds to a least squares approximation.

The reconstructions were also used to study the individual variability and the topographic order of the cortical maps. To allow comparison across animals, we defined 25 corresponding locations within the estimated maps having the same RF centers on the paw in each individual experiment. The average positions of the cortical representations of these selected locations on the paw were calculated in stereotaxic coordinates. In a subsequent step, the locations were normalized for the absolute cortical position in the individual maps (into "position-corrected" coordinates) using the centers of the individual representations as coordinate system origin. For further exploration of factors contributing to the overall variability, cortical coordinates were corrected for both position and representational extent by normalizing to the rostrocaudal (0–1.5) and mediolateral (0–1) extents of individual maps after correcting for position (resulting in "extent-corrected" coordinates). These ranges were chosen to match the average size of the cortical representations of each individual experiment (mean values 1.03 mm mediolaterally and 1.47 mm rostrocaudally) and the corresponding length-width ratio (mean value 1.53).

For all three types of coordinate systems, the absolute mean deviations in position with respect to the average positions of the cortical representations of the selected points on the paw were used as a measure for variability. While the first approach (uncorrected stereotaxic coordinates) provided information about the overall variability present in the cortical maps, position-corrected maps served to eliminate the component caused by a different localization in terms of stereotaxic coordinates. Further correction for the areal extent of the maps was intended to cancel the influence of differences in the size of the representational maps, thus leaving those components caused by the variability and scatter of the internal layout of the maps.

To estimate topographic orderliness in representational maps quantitatively, we calculated the degree of distortion of the initially rectilinear grid overlaying the hindpaw by computing the angles present at nodes of the projected grid on the cortical surface. Using the circular standard deviations of angles in masks covering a surface of 1/100 of the extent of each individual cortical representation, we obtained a measure for local orderliness.

Statistical analysis

For comparisons of data groups, Mann-Whitney and Wilcoxon tests (both two-tailed) were employed. Deviations and error bars represent standard errors of the means. Correlation analysis was applied by means of Spearman's correlation coefficient combined with a t-test procedure. Where values are represented as local means within defined intervals of the independent variable, all data points were used for associated correlation analyses. Where data were plotted against the rostrocaudal cortical axis, this coordinate was normalized on the total rostrocaudal extent of the representation in the individual experiments.

Histology

In a number of experiments, histological reconstructions were made to ascertain the reliability of microelectrode placement. Chicago sky blue was iontophoretically applied with a constant current (via a WPI A365 stimulus isolator) of 10 μA for 5–10 min. After sacrificing the animals by intracardial administration of an overdose of anesthetic, the brains were removed and fixated in formalin (10%) and later transferred to formalin (10%)-sucrose (15%) to compensate for volume changes. Frozen sections were cut and stained with neutral red (Merck).

Results

We investigated the laminar specificity of receptive fields (RFs) and of cortical representational maps of the hindpaw representation. For the present analysis, a total of 308 RFs in layer II/III, 501 RFs in layer IV, and 425 RFs in layer V were recorded in 502 penetrations in the hindpaw representation of somatosensory cortex in 29 adult rats. Mapping of the hindpaw representation in layers II/III, IV, and V revealed systematic differences between these

laminar groups at the level of RFs and related geometric properties such as position and overlap, but relatively little evidence for systematic layer specificities in parameters extracted at the level of entire representations.

RF size

Examples of RFs derived in a typical experiment in different cortical layers at various locations in the hindpaw representation are illustrated in Fig. 1. The distribution of RF sizes projected onto the cortical surface shows qualitatively that RF size can differ considerably within a single map of the hindpaw for a given layer as well as across layers (Fig. 1A).

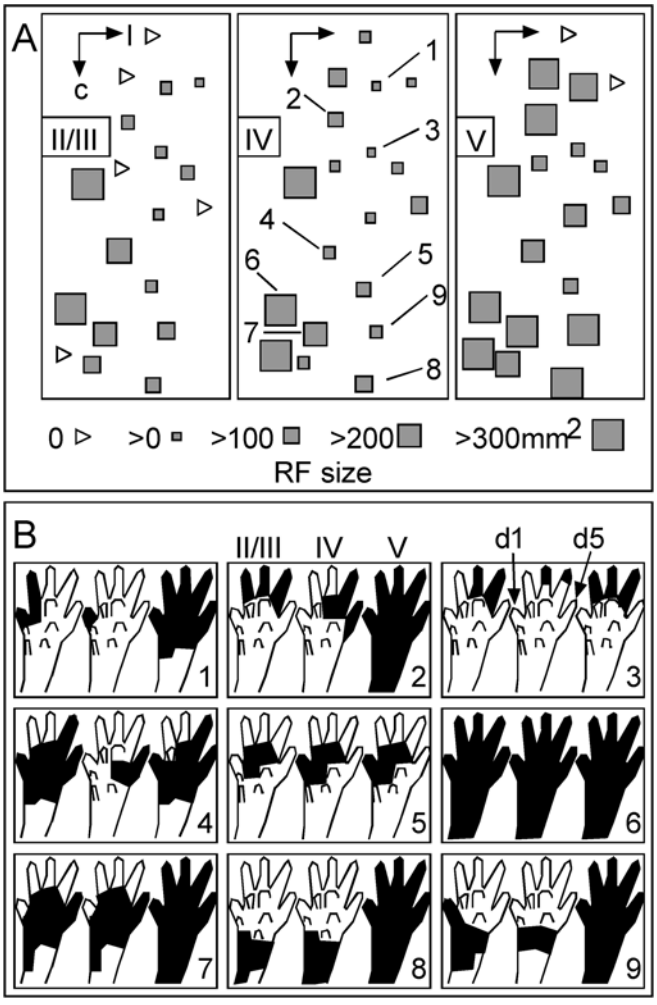

Fig. 1 A Distribution of RF sizes within the cortical SI hindpaw representation from one representative experiment (*II/III* supragranular layer, *IV* granular layer IV, *V* infragranular layer). *Scale bars* 0.2 mm (*c* caudal, *l* lateral). *Each symbol* corresponds to a recording site from perpendicular penetrations. *Open triangle* indicates unresponsive site; *squares of different sizes* indicate RF size according to the *inset*. *Numbers* refer to recording sites whose RF outlines are depicted in the figurines of the hindpaw in **B**. **B** RFs (*black regions*) on the hindpaw encountered during individual vertical penetrations in layers II/III, IV, and V (corresponding to numbered recording sites marked in **A**)

Given our handplotting criterion, cutaneous RFs usually contained at least one digit or one pad, but frequently a larger surface on the paw. This finding holds for all layers (Fig. 1B). The digit representation was located rostrolaterally. Digits d1 to d5 were mapped from medial to lateral; more proximal parts of the hindpaw were represented in the caudal section of the cortical map. We found that the gross topography was preserved across all layers. In extragranular layers, the topography of the hindpaw representation was less clear because of the large RFs, especially in layer V: RFs recorded in laminar V at sites 2, 6, 7, 8, and 9 included responses elicited by stimulation of any site on the glabrous surface of the paw (Fig. 1B). Such RFs were distributed over the entire extent of the hindpaw representation. Even in layer IV, neighborhood relationships were not always strictly preserved. This is illustrated by RFs of sites 2 and 3 (Fig. 1B), where the rostrocaudal and the mediolateral somatotopic gradient was not reflected in an equivalent shift of the positions of the centers of the corresponding RFs on the paw.

The laminar differences implied by individual penetrations were corroborated by comparison of the average RF sizes obtained for each layer. For infragranular layers, mean RF size was 161±4.6 mm^2 (n=425), 87±3.7 mm^2 for supragranular RFs (n=308), and 71±2.8 mm^2 in layer IV (n=501). All laminar groups differed significantly from each other (P<0.01 in all cases).

The broad range of RF sizes encountered in each laminar group is illustrated by the frequency distributions (Fig. 2). RF sizes varied considerably: in layers II/III and IV, the smallest RFs extended over about 10 mm^2, while the largest RFs found covered the entire glabrous skin surface of the hindpaw (345 mm^2). In layer V, very large RFs were found more frequently than in the other layers.

Unresponsive sites were occasionally encountered within the cutaneous representation of the hindpaw. Such sites were more common in the supragranular layers (Fig. 1A). In contrast, unresponsive locations were only rarely seen in layer IV (one in 502 penetrations). For a given penetration, we found no reliable cutaneous responses in extragranular layers if there were no RFs in layer IV.

To rule out that spontaneous fluctuations of RF size occurring during our experiments lasting usually up to 2 h might have obscured the laminar specificity reported, we remapped RFs in three animals 2–4 h after completion of the first mapping. Mean individual differences resulting from comparing RFs mapped the first and second time were small (−4.82±3.91 mm^2, n=39, layers II/III; 0.27 ±2.07 mm^2, n=93, layer IV; and −3.66±6.89 mm^2, n=70, layer V). Normalized on the initial RF size, we found that the spontaneous fluctuations were in the range of 5.85 ±7.53%, 1.74±3.12%, and 6.04±6.47%, layers II/III, IV, and V respectively. These data demonstrate that spontaneous changes of RFs observed over a time period of several hours were comparatively small.

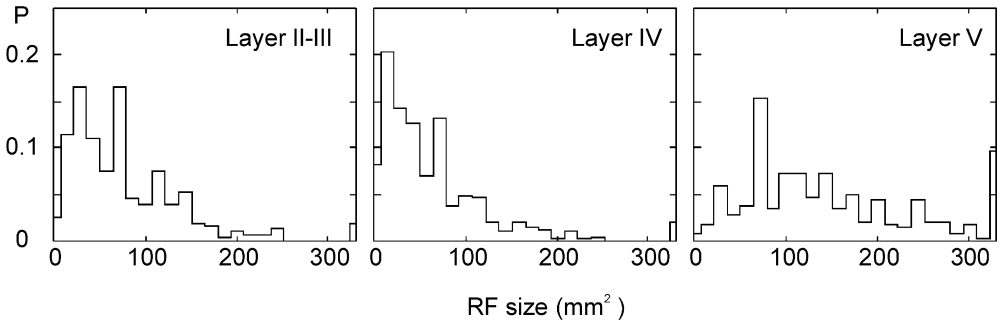

Fig. 2 Normalized frequency distributions of RF size based on 308 recorded RFs in layer II/III, 501 RFs in layer IV, and 425 RFs in layer V

RF overlap across layers

RFs recorded in individual vertical penetrations overlapped to an extensive degree, but their centers were not necessarily located at identical skin positions. The qualitative relation between RFs measured in individual penetrations was studied by calculating the ratios of RF sizes between all three layers recorded from, with RFs in layer IV as reference (Fig. 3A). The ratios for RFs of layers II/III–IV and layers V–IV were highly correlated independent of the position of RFs on the hindpaw. Accordingly, for single vertical penetrations, RFs were largest in layer V and smallest in layer IV. Other configurations were less frequently observed: in some cases, supragranular RFs were smaller than those in layer IV. On average, supragranular RFs were 1.8 times larger than fields in layer IV. For comparison, infragranular RFs were 3.45 times larger than layer IV RFs.

As a next step we calculated the relative overlaps of RFs within each vertical penetration (Fig. 3B). This analysis provides further information about the mutual positioning of RFs recorded in a single penetration with respect to each other. The normalized average overlaps with layer IV as reference were very high for RFs of layer II/III (86.5 ±1.4%). Average overlaps were even higher for layer IV RFs with layer V (96.1±0.8%). Using layer II/III as reference, we also found a high overlap with layer V (88.4 ±1.5%), but there was a less pronounced overlap with layer IV (69.8±1.8%). With layer V RFs for reference, overlaps were smaller with both supragranular (56.6 ±3.4%) and layer IV RFs (47.9±1.4%). Accordingly, RFs across all layers were generally completely contained within the largest RF encountered during a single vertical penetration. To some extent, this analysis reflects the size differences of RFs described above: RFs in layer IV were contained within the RFs in layer II/III, which in turn were contained in the RFs of layer V. As a rule, layer IV RFs were almost always completely contained within their layer V counterparts.

RF scatter

To provide an estimate about the scatter of the locations of RFs found in a single penetration across laminar groups, we computed the distance of pairs of RF centers for every possible laminar comparison. Figure 4 shows an example of the RF scatter for a typical experiment for all penetrations for each pair of laminar groups.

Dependent on the location, a scatter up to several millimeters was found. This finding was confirmed by computing the average distances for all penetrations in all experiments. The average scatter was 2.14±0.15 mm between layers II/III and IV, 3.14±0.20 mm between layers V and IV, and 3.07±0.19 mm between layers V and II/III (12 animals, n=175 penetrations). Accordingly, the scatter found between layers II/III and IV was smaller than that found in relation with layer V (P<0.01 for both comparisons). When the average scatter was plotted as a function of the rostrocaudal extent of the hindpaw map (Fig. 4), we found a significant dependence on cortical position for scatter between layer V and IV (Spearman's coefficient −0.128, P=0.029).

Response planes

To provide a quantitative estimate and an objective measure of RF size for comparison, we recorded response planes according to the technique described in Godde et al. (1996). A total of 15 response planes were obtained in 3 animals. Figure 5 shows examples recorded in a perpendicular penetration together with the RFs determined by handplotting. The quantitative measurements confirmed the small size of RFs in layer IV characterized by steep profiles yielding very sharply defined RF centers. The extent of RFs in the supragranular layers was much more variable. Response planes of layer II/III RFs differed from layer IV in that they had more flattened profiles, sometimes with multiple peaks of low amplitude above adjacent regions of the RF. At infragranular recording locations, RFs were larger than in supragranular recordings and the response profiles were even broader, indicating the less distinct response behavior. In general, comparison between RF dimensions determined by response planes and by handplotting revealed a profound correspondence. However, for all RFs for all laminae RFs delineated by handplotting were generally smaller.

RF gradient

A major source of variation of RF size within a given layer was the position of the RF within the hindpaw

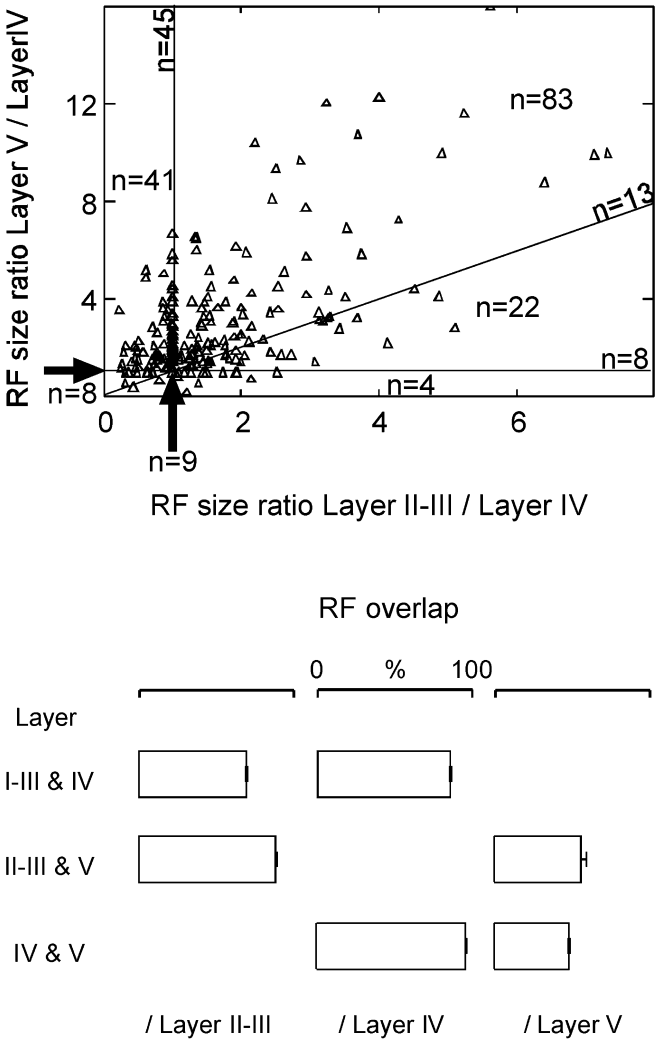

Fig. 3 *Top* Correlation between RF sizes and laminar groups recorded in single penetrations. RF sizes in supra- and infragranular layers are normalized on the layer IV RF for each corresponding penetration to show the laminar relationships of RF sizes. Spearman's correlation coefficient is 0.49 ($P<0.01$). The *numbers* correspond to the number of data points in each section of the plot delimited by, or laying on, the lines $x=y$, $x=1$, and $y=1$. In the remaining sections where no numbers are given, $n=0$ or 1. Lines are $x=1$, $y=1$, and $x=y$. For $x=1$, RF size is the same in layers II/III and IV. For $y=1$, RF size is the same in layers IV and V. For $y=x$, the RF size is the same in layers II/III and V. The areas delimited by these lines are conditions where RF sizes differ between all laminar groups. The most common condition is $y>x$ and $y>1$ and $x>1$; this corresponds to RF sizes smallest in layer IV and largest in layer V. The total number of data points (RF tripels) is 236. *Bottom* Relative RF overlaps between RFs from different layers recorded in individual penetrations, pooled across all penetrations and experiments. The laminar group whose RF was used for normalization is marked for reference on the bottom. Comparison revealed significant differences ($P<0.01$) for all cases except for overlaps between layers II/III and layer IV (reference layer IV) and layers II/III and layer V (reference layers II/III). Number of overlaps was $n=306$ for layers II–III and IV, $n=269$ for layers II–III and V, and $n=424$ for layers IV and V

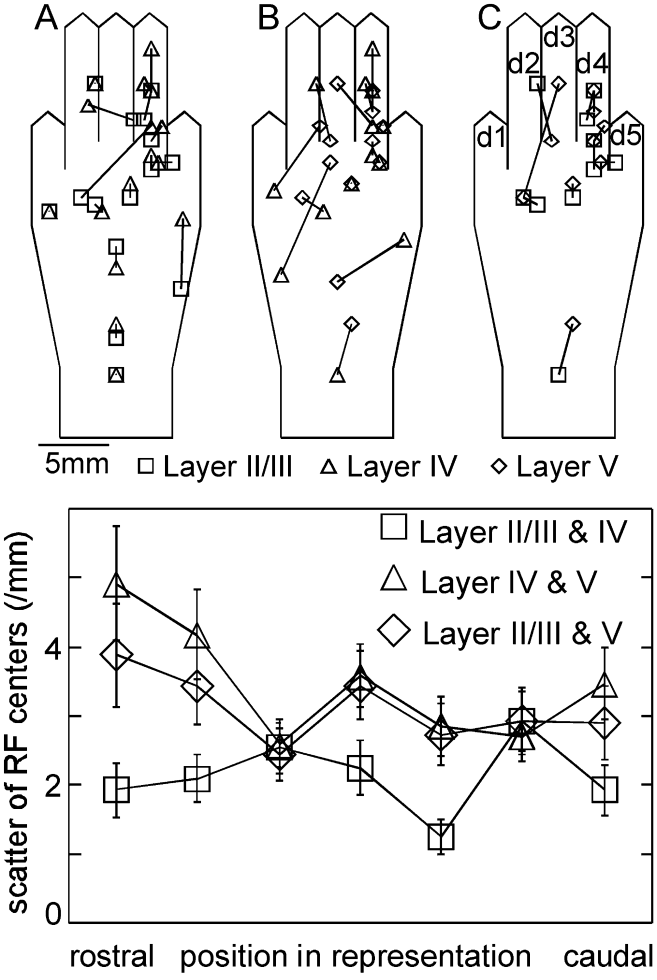

Fig. 4A–C Scatter of RF centers for RFs recorded in different layers in individual penetrations. *Top* Scatter of RF centers on the skin surface between layers II/III and IV; **B** between layers IV and V; **C** between layers II/III and V, pairs are connected with *a line,* and *symbols* indicate the layers the RF was recorded from. *Scale bar* 5 mm. *Bottom* Average scatter (±SEM) of RF centers as a function of the rostrocaudal extent of the hindpaw representation

representation. RFs were larger in proximal regions of the hindpaw map as compared to the more distal aspects. Rostrally, RFs recorded in supragranular layers and in layer IV were similar in size. In supragranular layers, but not in layer IV, RFs increased continuously in size towards the caudal portion.

This gradient could be observed in individual experiments for all laminar groups (Fig. 1B). The size differences between the infragranular and the other layers were maintained (Fig. 6). On the other hand, the gradient obscured differences between layer IV and II/III RFs. For example, layer IV RFs recorded at the caudal extent were larger than layer II/III RFs recorded at the rostral locations. The correlation strength between RF size and the rostrocaudal axis within the hindpaw representation was similar in layers II/III and IV, but weaker in layer V [Spearman's correlation coefficients: 0.377, 0.344, and 0.183 ($P<0.01$) for layers II/III, IV, and V respectively; data from 17 experiments].

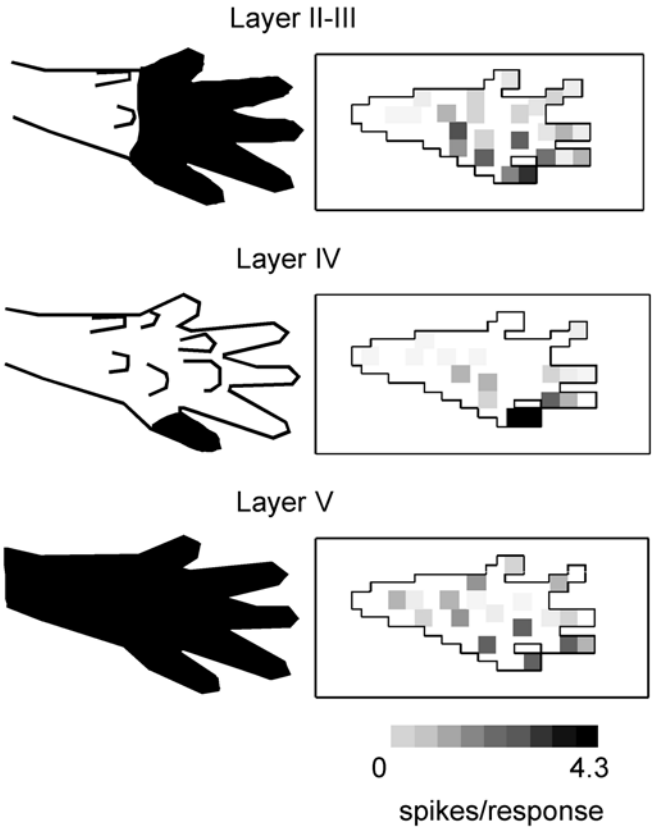

Fig. 5 Comparison of RFs as determined by handplotting (*left*) and PSTHs with subsequent construction of response planes based on computer-controlled stimulation of 20 different skin locations (*right*). Response strength (spikes per accumulated response, number of trials = 32) obtained from PSTH responses measured for each location are marked in a schematic drawing of the hindpaw at the respective location by *gray level coding* as shown at the bottom

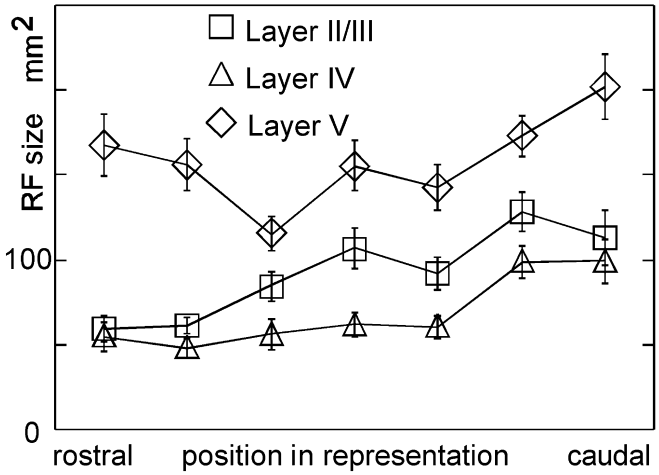

Fig. 6 Average RF sizes (±SEM) in the normalized rostrocaudal coordinate of the cortical hindpaw representation. Spearman's correlation coefficients are 0.377, 0.344, and 0.183 ($P<0.01$) for layers II/III, IV, and V respectively. Data from 17 experiments

Cortical maps

The topography of cortical maps of the hindpaw representation was studied by a quantitative reconstruction method taking into account the geometric centers of RFs and the corresponding cortical recording locations. Examples of maps obtained from the different layers in two individual experiments are shown in Fig. 7A, B. The RF centers and the grids are also displayed in the source space (paw) for reference. The map of layer IV shown in Fig. 7A is characterized by a very orderly representation, containing an almost complete map of the hindpaw. In contrast, the layer V map reconstructed from penetrations of the same animal revealed a highly incomplete map. The incompleteness is largely due to the fact that the centers of layer V RFs were located within a restricted portion of the hindpaw representation. Note that the dotted lines showing the outline of the paw are from extrapolation to provide an overview of the entire paw for visualization.

Deformations of an orderly and accurate topography can be inferred from distortions of the rectangularity of the grids. As shown in Fig. 7A, such distortions were present in all layers, but to a variable degree. We typically found a larger mesh size of the grid for the distal parts of the hindpaw, indicating an overrepresentation of these skin portions.

In contrast to the examples shown in Fig. 7A, the maps shown in Fig. 7B were characterized by less well-preserved topographies for all layers. The disorder was most severe in layer V. Despite these severe map distortions, the overall orientation of the proximodistal paw axis was comparable across layers, but rotated away from orthogonality with the stereotaxic coordinates.

Average cortical maps of the hindpaw obtained from 12 individual maps are shown in Fig. 8. The main purpose of these maps was to study variability as described in the next section. The layout of such maps was comparable to those obtained from individual experiments, but smaller in extent, because of the individual variability. In extra-granular layers, differences between average and individual maps appeared to be less pronounced, while the average map of layer IV differed considerably from the individual maps, indicating that layer IV in particular might be subject to interindividual variability.

Cortical map variability

For further analysis of map scatter and variability, we calculated the absolute mean deviations of cortical locations representing the same points on the hindpaw in individual experiments (Fig. 9A). The maximum deviations, and thus overall map variability, were in the order of 0.4 mm in all laminar groups. In extragranular layers, the spatial scatter of a point in the cortical representation was correlated with its position along the proximodistal axis of the hindpaw (Spearman's coefficients in layers II/III 0.21 and in layer V 0.25, $P<0.01$).

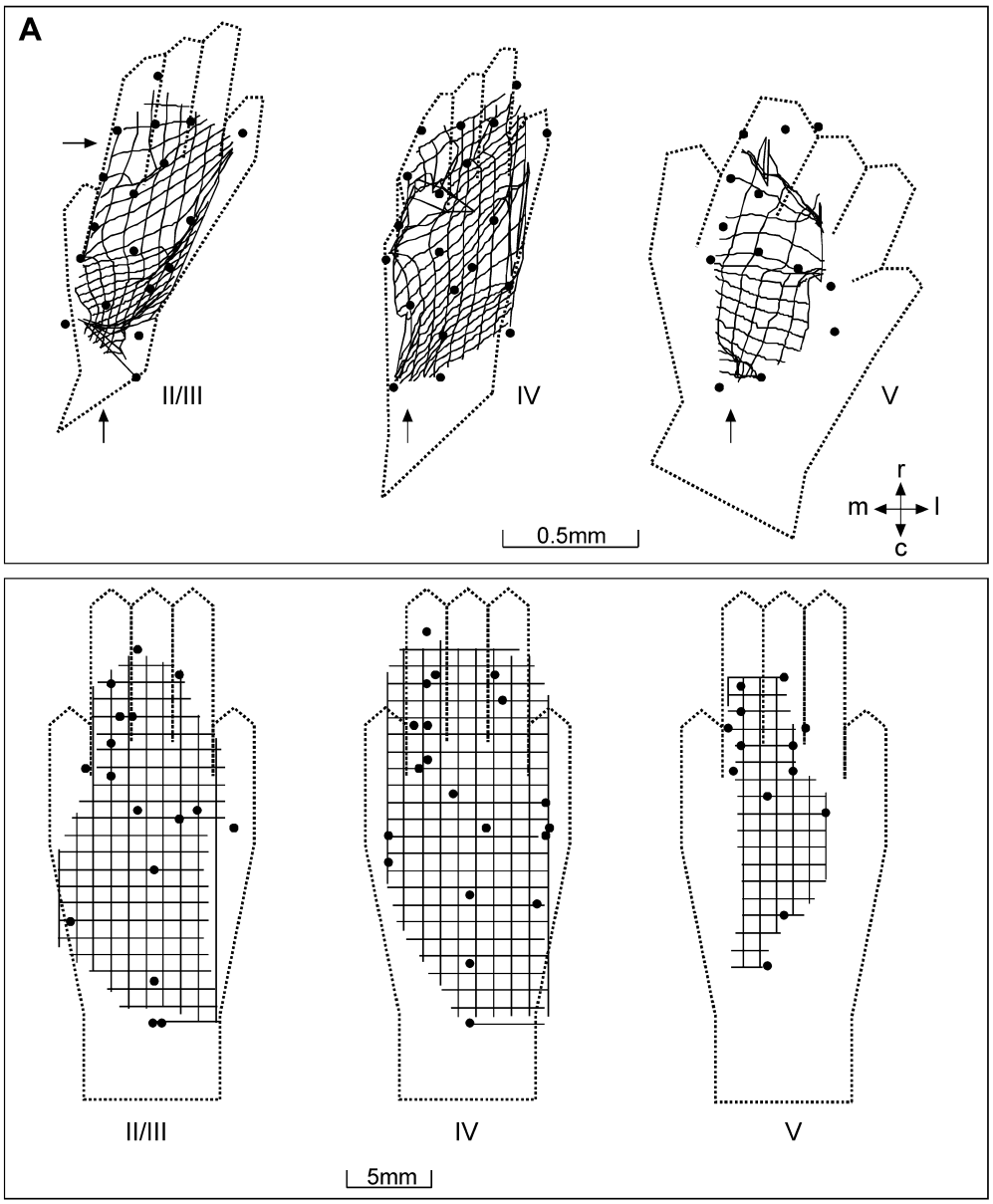

Fig. 7A, B Computer-based reconstruction of cortical maps of the hindpaw by interpolation of geometric RF centers and the cortical coordinates of corresponding penetration sites using data from layers II/III, IV, and V. *Top panels* depict the computed cortical map reconstructions as a grid (mesh size corresponds to 1 mm in skin space), the *dotted lines* show the outline of the paw as obtained from extrapolation that is provided only to assist in relating the position and orientation of the reconstructed map to the hindpaw (*m* medial, *l* lateral, *r* rostral, *c* caudal). *Scale bar* 0.5 mm; *perpendicular arrows* indicate position of Bregma; *horizontal arrow* 2.6 mm lateral. Digits d1–d5 are represented from medial to lateral. Penetration sites are indicated by *filled circles*. *Bottom panels* show the RF center locations (*filled circles*) and the grid used for mapping on the hindpaw. **A** Typical example from an individual experiment. **B** Example where distortions of topography were apparent

As a next step, we excluded "cortical location" as a source of variability. As a result of the normalization, variability was reduced by about 50% as compared to the uncorrected maps. After correction, average deviations were 0.21–0.26 mm (Fig. 9A). Only under these conditions did variability exhibit a significant laminar specificity. Corrected map variability was lowest in layers II/III and highest in layer IV. In layers IV and V we observed a significant correlation between map variability and the corresponding locations along the proximodistal coordinates of the hindpaw (Spearman's coefficients 0.56 and 0.31, $P<0.01$ in both cases). Accordingly, other factors such as the extent of individual maps and their internal layout are likely to contribute to the overall map variability.

The contribution of the spatial extent, i.e. the size of individual maps, was removed by an additional normalization. Generally, variability normalized for size was further reduced, indicating that size contributed to a minor extent. In detail, variability normalized for size of the supragranular maps was lower than that of the other, deeper laminar groups (0.21 coordinate units on average versus 0.25 in layers IV and V, $P<0.01$). In addition, as illustrated in Fig. 9B, we found a significant correlation between variability and the corresponding positions along the proximodistal hindpaw coordinates in all laminar groups (Spearman's coefficients for layers II/III 0.35, layer IV 0.76 and layer V 0.37, $P<0.01$).

Topographic order

Another aspect related to map variability is the internal order of representational topography. We assumed that the circular standard deviations of angles in the reconstructed map grid are negatively correlated with local orderliness of

Fig. 7A, B (continued)

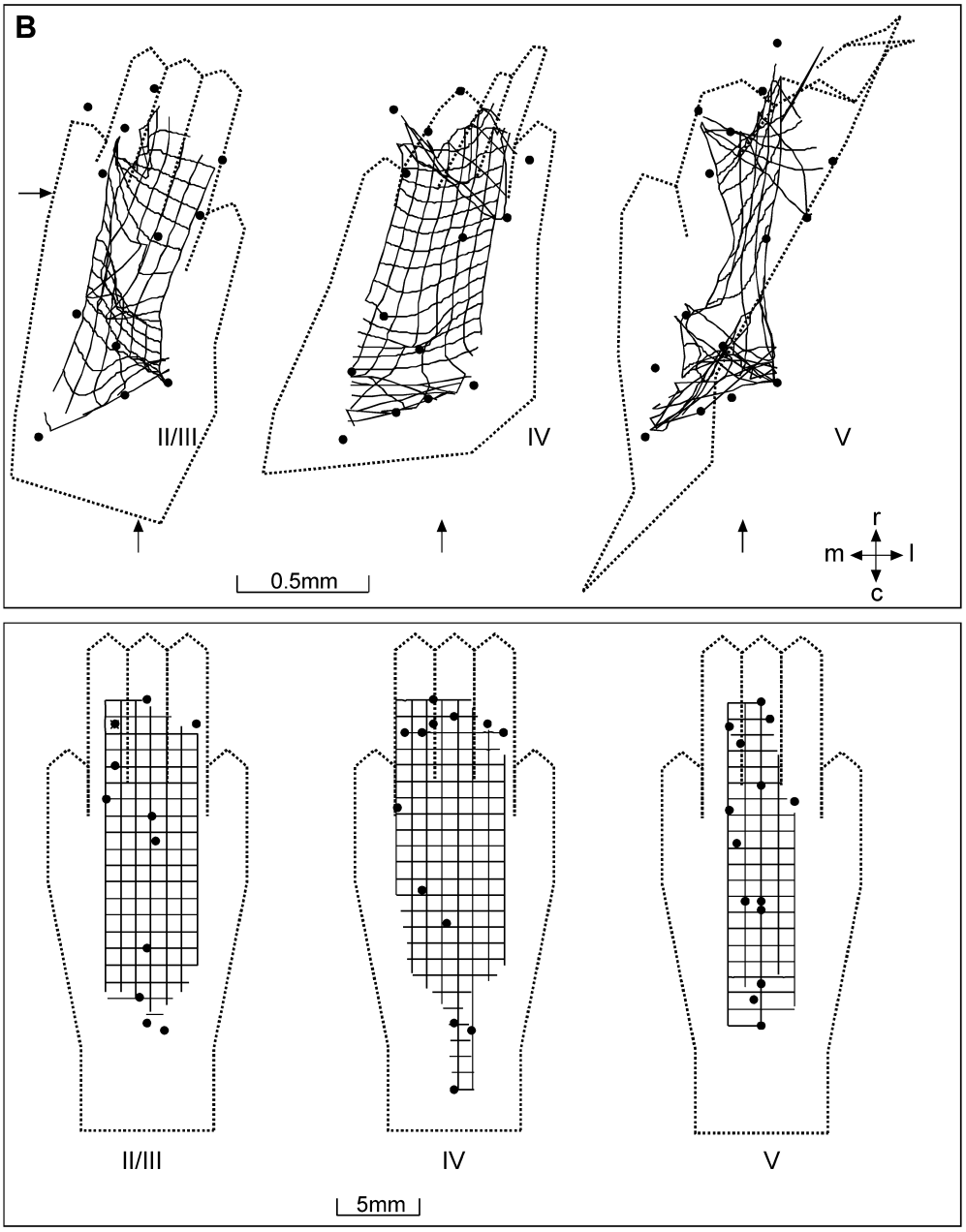

topography. Local means of these standard deviations were plotted as a function of the rostrocaudal cortical coordinate (Fig. 10). In layer IV, orderliness defined as above was strongly correlated with the rostrocaudal extent, i.e. the orderliness was lower in the digit representation than in the more caudal parts of the hindpaw representation (Spearman's coefficient −0.494, $P<0.01$). For the two other laminar groups, such a clear relationship was not found, but was present in some individual maps. For average layer V maps, lowest orderliness was found both rostrally in the digit portions of the map and in the center of the representations, a finding more frequently seen in the individual maps. Orderliness was not different between layers II/III and IV, but significantly lower in layer V ($P<0.01$).

Discussion

We performed a comparative mapping study in different laminar groups in the hindpaw representation of the rat somatosensory cortex (SI). The study intended to provide a quantitative description in layers II/III, IV, and V of the topography of the hindpaw map based on RF size, position, scatter and overlap on the one hand, and on parameters encompassing the entire cortical maps on the other hand such as their internal order and individual variability. We found substantial layer-specific differences, but provide also evidence for a considerable variability within and across layers. Even at the level of entire representational maps, a considerable degree of individual variability with little evidence of distinct laminar differences was apparent. While RF properties were subject to a

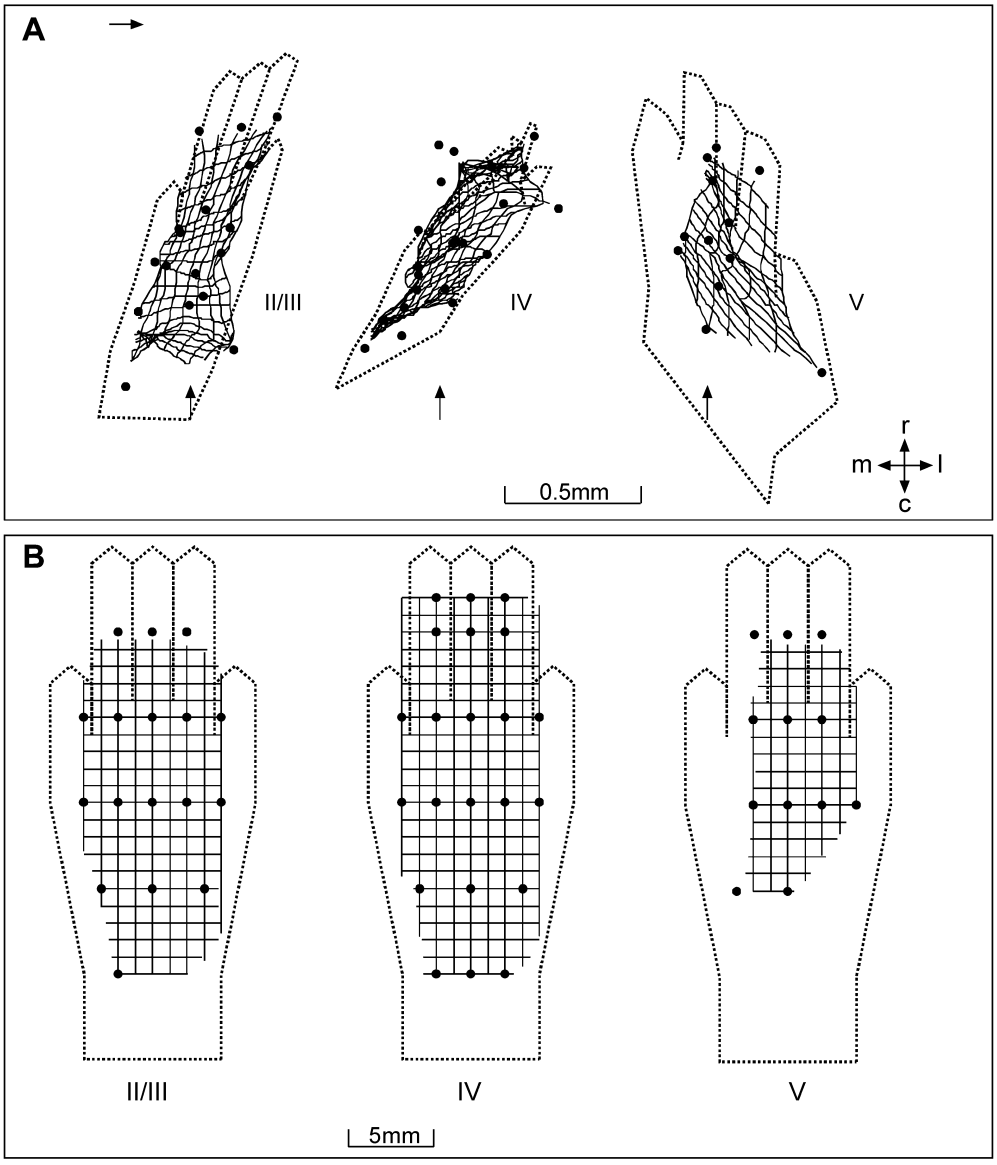

Fig. 8A, B Average hindpaw representations for layers II/III, IV and V (data from 12 experiments). Same conventions as in Fig. 7. The cortical locations corresponding to 25 identical locations on the paw were selected within each individual reconstructed map and used for averaging across animals

number of studies investigating layer-specificity of cortical processing, there is so far no analysis devoted to a laminar comparison at a representational level.

Receptive field size

Studies performed in rat and mouse somatosensory cortex described clear layer-specific differences of RF size (Simons 1978; Simons and Woolsey 1979; Lamour et al. 1983a; Chapin 1986). Our findings are in line with the notion that the smallest RFs are found in layer IV, that RFs in layer II/III are larger, but that largest RFs are typically found in infragranular layers. Yet, there appear to be many exceptions, for example, Dykes and Lamour reported a subpopulation of small RFs in infragranular layers (1988).

Laminar differences can be interpreted with respect to differences in afferent inputs and functional connectivity of cells and cell types according to laminar location. In this view, differences in RF size might be attributable to different morphological cell types (Simons 1978; Simons and Carvell 1989; Armstrong-James et al. 1992; Welker et al. 1993). Due to massive intracortical connectivity, layer V neurons receive inputs from all other layers via extensive branching of their basilar and apical dendrites (Killackey et al. 1989; Koralek et al. 1990), providing an explanation for the large size of infragranular RFs.

Receptive field scatter

The precision of the columnar organization is among other things limited by the intracolumnar scatter of RF position. According to our data, RF scatter defined as the distance of pairs of RF centers for every possible laminar comparison in individual penetrations is in the range of 2–3 mm. Given an average RF size of 60 mm^2 in the rostral portion of the digit representation, and assuming a

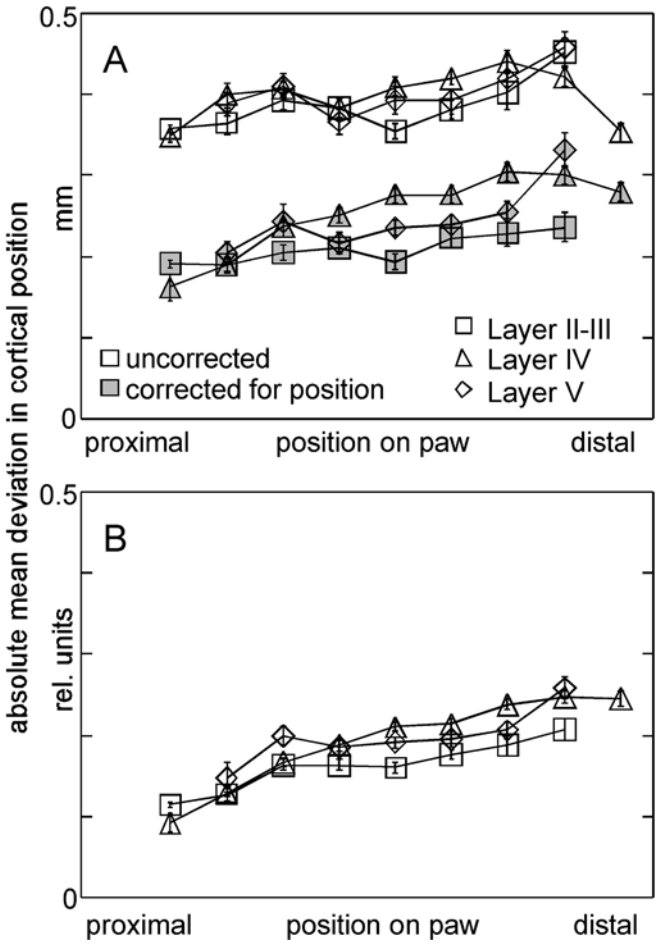

Fig. 9A, B Absolute mean deviation of individual reconstructed cortical maps from average maps (12 experiments) versus position along the proximodistal extent of the paw. **A** Deviations for uncorrected cortical coordinates (*open symbols*) and for cortical coordinates corrected for cortical position of the individual representations (*gray symbols*). **B** Deviations for cortical coordinates corrected for position and rostrocaudal and mediolateral extents of the individual representations

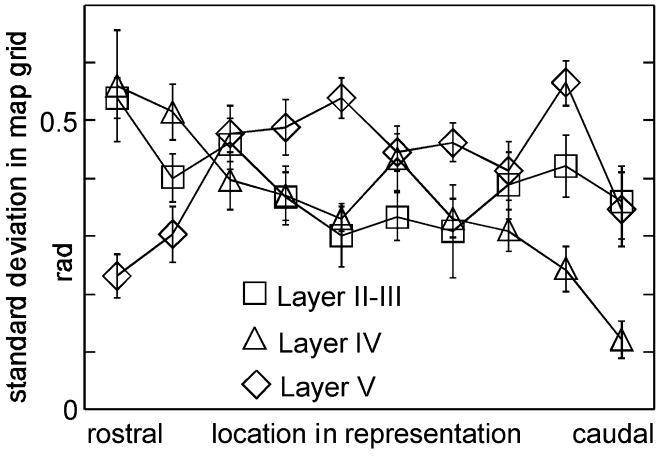

Fig. 10 Local means of standard deviations of angles in the reconstructed map grid on the cortical surface in relation to the rostrocaudal extent of the cortical hindpaw representation; data from 13 experiments. Higher deviations represent lower orderliness in the map

circular shape of RFs, this value corresponds to a mean diameter of about 9 mm. Consequently, RF scatter is in the range of 25–30% of the RF diameter. For the central 20 deg visual field representation of cat visual cortex (area 17), an average RF scatter of at least 50% of the average RF diameter has been reported (Albus 1975). According to these data, average scatter in terms of RF size is similar or smaller in the paw representation of SI as compared to the central visual field representation in cat area 17.

Handplotting versus quantitatively assessed RF profiles

Application of quantitative approaches to define RF profiles was advocated many years ago (Stevens and Gerstein 1976); the "response plane technique" is now widely used in visual and auditory systems. Technically, the application of comparable techniques is somewhat more difficult in tactile modalities (e.g. Chapin 1986; Johnson and Phillips 1988; Gardner and Palmer 1989). There is always a trade-off between the time-consuming quantitative approaches yielding a limited number of cells and qualitative methods allowing a much higher number of neurons to be sampled. We favored the second approach to be able to perform a laminar comparison on the level of RFs and cortical maps. Recently, Schlüter and coworkers (2001) described a strong correlation between RF sizes determined by handplotting and by response planes. As a rule, RF size was constantly underestimated by handplotting by about 50%, which is most likely due to the heavy trial averaging performed in response plane techniques. This comparison indicates that handplotting provides reliable and reproducible information about RF size and location given that constant criteria are used.

Regional differences in RF size

In addition to the laminar position, RFs within the hindpaw representation cover different skin portions such as digits, pads or the heel. RF size varied significantly between those skin regions giving rise to a profound rostrocaudal gradient, which we referred to as regional differences in RF size. According to our study, regional differences are present in all layers tested and can obscure laminar differences in RF size (Fig. 5).

In the barrel field of rats, arbors of thalamocortical axons can span areas of almost 1×0.5 mm (Jensen and Killackey 1987). A constant number of relay cells per cortical surface have been shown to project to each subdivision of SI (Saporta and Kruger 1977), suggesting a similar innervation density. In that case, the synaptic weights of the afferents on their cortical targets in combination with intracortical mechanisms are likely candidates that establish the gradient in RF size observed. Moreover, the range of inhibition, which controls RF size, could be variable within the representation.

Spontaneous fluctuations of RF size

In both awake and anesthetized preparations, ongoing fluctuations of neural responsiveness are a typical feature (Arieli et al. 1996; Nicolelis et al. 1998). To provide stable states of anesthesia over longer periods of experimentation, urethane is commonly used in physiological experiments because of its stability (Maggi and Melli 1986; Armstrong-James and George 1988). However, cortical and subcortical responsiveness to sensory stimulation has been shown to clearly depend on the depth of anesthesia (Chapin and Lin 1984; Friedberg et al. 1999; Kisley and Gerstein 1999; Erchova et al. 2002). In our experiments, according to respiratory rates and heart rates recorded together with the presence of different reflexes monitored during our experiments, the typical anesthetic levels might have corresponded to levels III 3 to 4 (Guedel 1920), although quite different rate ranges have been used to allocate an anesthetic level (cf. Friedberg et al. 1999; Erchova et al. 2002). A striking increase in RF size from stage III 3 to III 2, but not between stages III 3 and III 4, has been shown for single units recorded from the ventral posterior medial thalamus (Friedberg et al. 1999). According to our data from the remapping experiments, spontaneous fluctuations arising from different anesthetic levels are rather small and therefore unlikely to cause or to obscure layer-specific differences at RF or representational levels.

Reconstruction of representational maps of the hindpaw

The representational maps generated by our reconstruction algorithm are in principle comparable to the qualitative maps described previously at lower resolutions (Welker 1971; Hall and Lindholm 1974; Chapin and Lin 1984). The interpolation algorithm we used is a modification of the approach initially introduced for the investigation of retinotopic maps in superior colliculus (Quevedo et al. 1996). As in the original version, we use the centers of RFs to obtain an interpolated map of the sensory surface. From a general point of view, topographic mapping implicitly assumes a point-to point relationship, which, given the dimensions of RFs, must always remain theoretical (cf. McIlwain 1983). However, even the simplest and spatially most restricted stimulus evokes fairly large and broad cortical activity areas (Grinvald et al. 1994; Godde et al. 1995; Chen-Bee and Frostig 1996). Accordingly, when considering real maps that inevitably are based on broad activation pattern, methods that do not rely on a bijective mapping are of considerable interest, i.e. that allow a mapping of a point (neuron) to an area (RF), or an area (activated cortex) to an area (RF).

Layer specificity of representational maps and average maps

To our knowledge, this is the first attempt to address lamina-specific features of entire representational maps. Supragranular maps generally resemble those in layer IV, whereas infragranular maps were often clearly different, reflecting the substantial laminar differences of RF size. However, interindividual variability of representational maps might outweigh possible laminar-specific features.

Distinct forms of interlaminar connections have been studied by HRP fiber tracing in rat visual cortex (Burkhalter 1989). Accordingly, geniculocortical input is processed through interlaminar connections that are topographically precise, widespread, or patchy. It was suggested that these connectivity patterns play a role for the transformation of functional maps between layers. Projections terminating in layers I to IV were speculated to transform functional maps, while the topographically precise projections found from upper to lower layers should preserve functional maps (Burkhalter 1989). According to our data, only layer V maps appear to show clear differences. This discrepancy might be due to the fact that infragranular cells with their broad apical and basal dendrites can integrate information over a much wider topographical area.

To quantify individual variability of representations, we computed average maps. The difficulties in combining data sets consisting of representational maps have been pointed out previously (Myasnikov et al. 1997). We agree that combinations of mapping data cannot define a unique high resolution prototypical map because of the inherently idiosyncratic nature of individual maps.

Map variability

We provided evidence that both the variability originating from stereotaxic coordinates, i.e. from differences in the absolute position on the cortical surface, and the variability originating from internal map layout are contributing in similar terms to the net map variability. In addition, map size appeared to contribute, but to a minor extent. Variability in position is likely to reflect variability of anatomical projection patterns (Lee and Woolsey 1975). The comparatively weak contribution of differences in the spatial extent of representations to the overall map variability can be interpreted in the light of recent findings showing how representational areas are alterable by the richness of sensory inputs (Coq and Xerri 1998; cf. Dinse and Merzenich 2002). As the animals used for our study are kept under highly standardized rearing conditions, our results showing little impact of spatial extent on overall map variability might reflect the constancy of the standard environment.

Anatomical variability contributing to differences in size of representations has been shown to be sensitive to the prenatal presence of afferent connections (Killackey et al. 1994). In fact, considerable anatomical variability in

size and lateral asymmetry of granular zones has been identified in rat SI cortex (Riddle and Purves 1995), with the whiskerpad representation differing by a factor of two. Similarly, a large variability in the size of single-whisker functional representations as measured by means of recording optically intrinsic signals has been reported that correlated weakly with the preferential use of the corresponding side of the sensory surface (Chen-Bee and Frostig 1996).

Variability of internal map topography is the second important component, which is also likely to reflect differences in sensory experience, both related to the individual itself in terms of preferential use, and to the richness of the environment. This component of variability displays a similar dependence on the skin position as described for RF sizes. According to our analysis, variability of internal map topography is highest in the representation of the digits, which is most heavily used.

The correlations between variability and position on the represented sensory surface were different for uncorrected, position-corrected, and maps corrected for both position and spatial extent. Notably positional variation appears to be more influential in layer IV than in other layers as variability is strongly correlated with position on the sensory surface in corrected maps but weakly in uncorrected data. This might be related to the existence of the most detailed topographies typically found in layer IV. In layer V, corrections have relatively little influence on correlation strength, while the spatial extent appears to play a role in layers II/III. Correlations between individual variability in maps and the position on the paw differ depending on the correction procedures applied to cortical coordinates. This implies that different components of variability are not having a spatially homogeneous impact.

Distributed processing across layers

Analyzing response latencies following sensory stimulation revealed that the layer-dependence of afferent inputs is reflected in differences of latency times (Best et al. 1986; Armstrong-James et al. 1992; Alloway et al. 1993), with the shortest latencies found in layer IV. There is agreement that sensory information entering layer IV is distributed across the other laminae giving rise to layer dependent delays (Best et al. 1986; Armstrong-James et al. 1992). However, response latency differences alone do not demonstrate a hierarchical step-by-step processing, where the proceeding stage waits until the end of the processing of a previous one. What must be taken into account additionally is response duration (Dinse 1994; Dinse and Krüger 1994). For tactile responses, the layer-to-layer accumulation in latency times is small (usually not exceeding 2–3 ms) compared to the overall response duration, which is in the range of about 20 ms (Armstrong-James et al. 1992; Dinse et al. 1997). Conceivably, by the time the cell finishes firing the information judged by latencies has been conveyed through all layers. What therefore seems more plausible is a continuous temporal interaction through which all layers are linked together. As a result, response properties recorded at a given layer do not merely reflect its laminar position, but also the outcome of the concerted action of the entire columnar system (Ghazanfar and Nicolelis 1999). In this view, similarities across layers might indicate a system of interactions between different layers. Extending this framework to entire representational maps, we suggest the mode of processing that encompasses both vertical and horizontal interactions to provide a single representation of entire body parts across layers.

Acknowledgements. We gratefully acknowledge the support of the Institute for Neuroinformatik. We thank Drs. G. Böhmer and B. Godde for critically reading drafts of the manuscript and to Dr. R. Necker for allowing us to do the histological processing in his lab. We are grateful to D. Möricke, M. Neef, M. Ziesmer and W. Dreckmann and the members of the machine shop for excellent technical support. S.S.H. is grateful to Professor S. Yoshizawa and to the late Professor K. Fukunishi for their support. The study was supported by the DFG (Di 334/10-1-3).

References

Albus K (1975) A quantitative study of the projection area of the central and the paracentral visual field in area 17 of the cat. I. The precision of the topography. Exp Brain Res 24:159–179

Alloway KD, Johnson MJ, Wallace MB (1993) Thalamocortical interactions in the somatosensory system: interpretation of latency and cross-correlation analyses. J Neurophysiol 70:892–908

Arieli A, Sterkin A, Grinvald A, Aertsen A (1996) Dynamics of ongoing activity: explanation of the large variability in evoked cortical responses. Science 273:1868–1871

Armstrong-James M, George MJ (1988) Influence of anesthesia on spontaneous activity and receptive field size of single units in rat Sm1 neocortex. Exp Neurol 99:369–387

Armstrong-James M, Fox K, Das-Gupta A (1992) Flow of excitation within rat barrel cortex on striking a single vibrissa. J Neurophysiol 68:1345–1358

Best J, Reuss S, Dinse HR (1986) Lamina-specific differences of visual latencies following photic stimulation in the cat striate cortex. Brain Res 385:356–360

Burkhalter A (1989) Intrinsic connections of rat primary visual cortex: laminar organization of axonal projections. J Comp Neurol 279:171–186

Carvell GE, Simons DJ (1990) Biometric analyses of vibrissal tactile discrimination in the rat. J Neurosci 10:2638–2648

Chapin JK (1986) Laminar differences in sizes, shapes, and response profiles of cutaneous RFs in the rat SI cortex. Exp Brain Res 229:549–559

Chapin JK, Lin CS (1984) Mapping the body representation in si cortex of anaesthetized and awake rats. J Comp Neurol 229:199–213

Chapin JK, Lin CS (1990) The somatic sensory cortex of the rat. In: Kolb B, Tees RC (eds) The cerebral cortex of the rat. MIT Press, Cambridge, MA, pp 341–380

Chen-Bee CH, Frostig RD (1996) Variability and interhemispheric asymmetry of single-whisker functional representations in rat barrel cortex. J Neurophysiol 76:884–894

Coq JO, Xerri C (1998) Environmental enrichment alters organizational features of the forepaw representation in the primary somatosensory cortex of adult rats. Exp Brain Res 121:191–204

Dinse HR (1994) A time-based approach towards cortical functions: neural mechanisms underlying dynamic aspects of information processing before and after postontogenetic plastic processes. Physica D 75:129–150

Dinse HR, Krüger K (1994) Timing of processing along the visual pathway in the cat. Neuroreport 5:893–897
Dinse HR, Merzenich MM (2002) Adaptation of inputs in the somatosensory system. In: Fahle M, Poggio T (eds) Perceptual learning. MIT Press, Cambridge, MA, pp 19–42
Dinse HR, Krüger K, Akhavan AC, Spengler F, Schöner G, Schreiner CE (1997) Low-frequency oscillations of visual, auditory and somatosensory cortical neurons evoked by sensory stimulation. Int J Psychophysiol 26:205–227
Donoghue JP, Kerman KL, Ebner FF (1979) Evidence for two organizational plans within the somatic sensory-motor cortex of the rat. J Comp Neurol 183:647–663
Dykes RW, Lamour Y (1988) An electrophysiological study of single somatosensory neurons in rat granular cortex serving the limbs: a laminar analysis. J Neurophysiol 60:703–724
Erchova IA, Lebedev MA, Diamond ME (2002) Somatosensory cortical neuronal population activity across states of anaesthesia. Eur J Neurosci 15:744–752
Friedberg MH, Lee SM, Ebner FF (1999) Modulation of receptive field properties of thalamic somatosensory neurons by the depth of anesthesia. J Neurophysiol 81:2243–2252
Gardner EP, Palmer CI (1989) Simulation of motion on the skin. I. Receptive fields and temporal frequency coding by cutaneous mechanoreceptors of OPTACON pulses delivered to the hand. J Neurophysiol 62:1410–1436
Gilbert CD (1977) Laminar differences in receptive field properties of cells in cat primary visual cortex. J Physiol (Lond) 268:391–421
Ghazanfar AA, Nicolelis MA (1999) Spatiotemporal properties of layer V neurons of the rat primary somatosensory cortex. Cereb Cortex 9:348–361
Godde B, Hilger T, von Seelen W, Berkefeld T, Dinse HR (1995) Optical recording of rat somatosensory cortex reveals representational overlap as a topographic principle. Neuroreport 7:24–28
Godde B, Spengler F, Dinse HR (1996) Associative pairing of tactile stimulation induces somatosensory cortical reorganization in rats and humans. Neuroreport 8:281–285
Grinvald A, Lieke EE, Frostig RD, Hildesheim R (1994) Cortical point-spread function and long-range lateral interactions revealed by real-time optical imaging of macaque monkey primary visual cortex. J Neurosci 14:2545–2568
Guedel AE (1920) Signs of inhalational anesthesia. A fundamental guide. In: Guedel AE (ed) Inhalational anesthesia. MacMillan, New York, pp 10–50
Hall RD, Lindholm EP (1974) Organization of motor and somatosensory neocortex in the albino rat. Brain Res 66:23–38
Henry GH, Harvey AR, Lund JS (1979) The afferent connections and laminar distribution of cells in the cat striate cortex. J Comp Neurol 187:725–744
Herkenham M (1980) Laminar organization of thalamic projections to the rat neocortex. Science 207:532–535
Jensen KF, Killackey HP (1987) Terminal arbors of axons projecting to the somatosensory cortex of adult rat: I. The normal morphology of specific thalamocortical afferents. J Neurosci 7:3529–3543
Johnson KO, Phillips JR (1988) A rotating drum stimulator for scanning embossed patterns and textures across the skin. J Neurosci Methods 22:221–231
Jones EG, Powell TP (1970) An electron microscopic study of the laminar pattern and mode of termination of afferent fibre pathways in the somatic sensory cortex of the cat. Philos Trans R Soc Lond B Biol Sci 257:45–62
Keller A, White EL, Cippolini PB (1985) The identification of thalamocortical axon terminals in barrels of mouse SmI cortex using immunohistochemistry of anterogradely transported lectin (*Phaseolus vulgaris*-leucoagglutinin). Brain Res 343:159–165
Killackey HP, Koralek KA, Chiaia NL, Rhodes RW (1989) Laminar and areal differences in the origin of the subcortical projection neurons of the rat somatosensory cortex. J Comp Neurol 282:428–445
Killackey HP, Chiaia NL, Bennett-Clarke CA, Eck M, Rhoades RW (1994) Peripheral influences on the size and organization of somatotopic representations in the fetal rat cortex. J Neurosci 14:1496–1506
Kisley MA, Gerstein GL (1999) Trial-to-trial variability and state-dependent modulation of auditory-evoked responses in cortex. J Neurosci 19:10451–10460
Koralek KA, Olavarria J, Killackey HP (1990) Areal and laminar organization of corticocortical projections in the rat somatosensory cortex. J Comp Neurol 299:133–150
Krone G, Mallot H, Palm G, Schüz A (1986) Spatiotemporal receptive fields: a dynamical model derived from cortical architectonics. Proc R Soc Lond B Biol Sci 226:421–444
Kyriazi HT, Simons DJ (1993) Thalamocortical response transformations in simulated whisker barrels. J Neurosci 13:1601–1615
Lamour Y, Guilbaud G, Willer JC (1983a) Rat somatosensory (SmI) cortex: II. Laminar and columnar organization of noxious and non-noxious inputs. Exp Brain Res 49:46–54
Lee KJ, Woolsey TA (1975) A proportional relationship between peripheral innervation density and cortical neuron number in the somatosensory system of the mouse. Brain Res 99:349–353
Maggi CA, Meli A (1986) Suitability of urethane anesthesia for physiopharmacological investigations in various systems. Part 1: General considerations. Experientia 42:109–114
McIlwain JT (1983) Representation of the visual streak in visuotopic maps of the cat's superior colliculus: influence of the mapping variable. Vision Res 23:507–516
Merzenich MM, Nelson RJ, Stryker MP, Cynader MS, Schoppmann A, Zook JM (1984) Somatosensory cortical map changes following digit amputation in adult monkeys. J Comp Neurol 224:591–605
Merzenich MM, Nelson RJ, Kaas JH, Stryker MP, Jenkins WM, Zook JM, Cynader MS, Schoppmann A (1987) Variability in hand surface representations in areas 3b and 1 in adult owl and squirrel monkeys. J Comp Neurol 258:281–296
Miller KD, Pinto DJ, Simons DJ (2001) Processing in layer 4 of the neocortical circuit: new insights from visual and somatosensory cortex. Curr Opin Neurobiol 11:488–497
Myasnikov AA, Dykes RW, Leclerc SS (1997) Correlating cytoarchitecture and function in cat primary somatosensory cortex: the challenge of individual differences. Brain Res 750:95–108
Nicolelis MA, Ghazanfar AA, Stambaugh CR, Oliveira LM, Laubach M, Chapin JK, Nelson RJ, Kaas JH (1998) Simultaneous encoding of tactile information by three primate cortical areas. Nat Neurosci 1:621–630
Quevedo C, Hoffmann KP, Husemann R, Distler C (1996) Overrepresentation of the central visual field in the superior colliculus of the pigmented and albino ferret. Vis Neurosci 13:627–638
Peters A, Jones EG (1984) Cerebral cortex, vol. 1. Plenum Press, New York
Recanzone GH, Merzenich MM, Dinse HR (1992) Expansion of the cortical representation of a specific skin field in primary somatosensory cortex by intracortical microstimulation. Cereb Cortex 2:181–196
Riddle DR, Purves D (1995) Individual variation and lateral asymmetry of the rat primary somatosensory cortex. J Neurosci 15:4184–4195
Rockel AJ, Hiorns RW, Powell TPS (1980) The basic uniformity in structure of the neocortex. Brain 103:221–244
Sanderson KJ, Welker WI, Shambes GM (1984) Reevaluation of motor cortex and of sensimotor overlap in cerebral cortex of albino rats. Brain Res 292:251–260
Saporta S, Kruger L (1977) The organization of thalamocortical relay neurons in the rat ventrobasal complex studied by the retrograde transport of horseradish peroxidase. J Comp Neurol 174:187–208
Schiller PH, Finlay BL, Volman SF (1976) Quantitative studies of single-cell monkey striate cortex. I. Spatiotemporal organization of receptive fields. J Neurophysiol 39:1288–1319

Schlüter O, Tissot L, Dinse HR (2001) Population analysis of plastic changes of rat somatosensory cortical neuron responses: peak position as a predictor for discrimination performance. Soc Neurosci Abstr 27:49.11

Schüz A, Miller R (2002) Cortical areas: unity and diversity: conceptual advances in brain research. Taylor and Francis, London (in press)

Sherman SM, Guillery RW (2001) Exploring the thalamus. Academic Press, San Diego

Simons DJ (1978) Response properties of vibrissa units in rat SI somatosensory neocortex. J Neurophysiol 41:798–820

Simons DJ, Carvell GE (1989) Thalamocortical response transformation in the rat vibrissa/barrel system. J Neurophysiol 61:311–330

Simons DJ, Woolsey TA (1979) Functional organization in mouse barrel cortex. Brain Res 165:327–332

Spengler F, Godde B, Dinse HR (1995) Effects of ageing on topographic organization of somatosensory cortex. Neuroreport 6:469–473

Stevens JK, Gerstein GL (1976) Spatiotemporal organization of cat lateral geniculate receptive fields. J Neurophysiol 39:213–238

Welker C (1971) Microelectrode delineation of fine grain somatotopic organization of SmI cerebral neocortex in albino rat. Brain Res 26:259–275

Welker E, Armstrong-James M, Van der Loos H, Kraftsik R (1993) The mode of activation of a barrel column: response properties of single units in the somatosensory cortex of the mouse upon whisker defection. Eur J Neurosci 5:691–712